Revision 1

Transition Metals in the Transition Zone: Crystal Chemistry of Minor Element Substitution in Wadsleyite

Li Zhang[1,2,*] Joseph R. Smyth[2] Julien Allaz[2] Takaaki Kawazoe[3] Steven D. Jacobsen[4] Zhenmin Jin[1]

[1] School of Earth Sciences, China University of Geosciences, Wuhan 430074, China.

[2] Department of Geological Sciences, University of Colorado, Boulder, CO 80309, U.S.A.

[3] Bayerisches Geoinstitut, University of Bayreuth, 95440 Bayreuth, Germany.

[4] Department of Earth and Planetary Sciences, Northwestern University, Evanston, Illinois 60208, U.S.A.

*Email:li.z.zhang@colorado.edu

ABSTRACT

As the most abundant solid phase at depths of 410 to 525 km, wadsleyite constitutes a large geochemical reservoir in the Earth. In order to better understand the implications of minor element substitution and cation ordering in wadsleyite, we have synthesized wadsleyites coexisting with pyroxenes with 2 to 3 wt% of either TiO_2, Cr_2O_3, V_2O_3, CoO, NiO, or ZnO under hydrous conditions in separate experiments at 1300 °C and 15 GPa. We have refined the crystal structures of these wadsleyites by single-crystal X-ray diffraction, analyzed the compositions by electron microprobe, and estimated M3 vacancy concentration from *b*/*a* cell-parameter ratios. According to the crystal structure refinements, Cr and V show strong preferences for M3 over M1 and M2 sites and significant substitution up to 2.7 % (atomic percent) at the tetrahedral site (T site). Ni, Co,

and Zn show site preferences similar to those of Fe with M1≈ M3 > M2 > T. The avoidance of Ni, Co, and Fe for the M2 site in both wadsleyite and olivine appears to be partially controlled by crystal field stabilization energy (CFSE). The estimated CFSE values of Ni^{2+}, Co^{2+}, and Zn^{2+} at three distinct octahedral sites show a positive correlation with octahedral occupancy ratios (M2/(M1+M3)). Ti substitutes primarily into the M3 octahedron, rather than M1, M2, or T sites. Ti, Cr, and V each have greater solubility in wadsleyite than in olivine. Therefore these transition metal cations may be enriched in a melt or an accessory phase if hydrous melting occurs on upward convection across the wadsleyite-olivine boundary and may be useful as indicators of high pressure origin.

Keywords: Wadsleyite, transition metals, X-ray diffraction, cation ordering

INTRODUCTION

Wadsleyite (β-Mg_2SiO_4) is a phase of very broad geochemical significance and is considered to be the fourth most abundant silicate phase in the Earth (after bridgmanite, olivine, and ringwoodite). The total mass of wadsleyite in the mantle may be more than four times the mass of the crust. High-pressure mineral-physics studies (Bolfan-Casanova et al. 2000; Demouchy et al. 2005; Kohlstedt et al. 1996) show that transition-zone minerals at average mantle temperatures have significantly higher water solubility (on the order of 1 wt% under realistic *T* and *P* conditions and as much as 3 wt%) than upper mantle minerals (less than 0.1- 0.2 wt.%), and as the ascending ambient mantle rises out of the high-water-solubility transition zone into the low-solubility upper mantle above 410 km, it may undergo dehydration-induced partial melting (Bercovici and Karato 2003). Unlike olivine, wadsleyite can also incorporate significant amounts of trivalent cations at both tetrahedral and octahedral sites (Bolfan-Casanova et al. 2012; Smyth et al. 2014). Therefore, minor element substitution in wadsleyite may have played a significant role in

the chemical evolution of the bulk silicate Earth. Substitution of hydrogen and transition metal cations in wadsleyite can influence the depth of wadsleyite-olivine boundary, and may result in hydrous melting at interface between transition zone and upper mantle (Woodland and Angel 1998; Kawamoto et al. 1996; Inoue et al. 2010; Deon et al. 2011; Bercovici and Karato 2003; Bolfan-Casanova et al. 2012).

Wadsleyite has the spinelloid III crystal structure (Akaogi et al. 1982) which is based on a cubic-close-packed array of oxygen anions. The structure (see Fig.1) is nominally orthorhombic (space group *Imma*), but can be slightly monoclinic (space group *I*2/*m*) with a beta angle up to 90.4° (Smyth et al. 1997). Wadsleyite has three symmetrically distinct divalent octahedral sites: M1 (4*a* position, point symmetry 2/*m*), M2 (4*e* position, point symmetry *mm*), and M3 (8*g* position, point symmetry 2), one tetrahedral site T (8*h* position with point symmetry *m*), and four distinct oxygen positions: O1 (4*e* position, point symmetry *mm*), O2 (4*e* position, point symmetry *mm*), O3 (8*h* position, point symmetry *m*), and O4 (16*j* general position). The tetrahedral sites form Si_2O_7 dimers and are unusually large with one of the longest Si-O distances of any pure silica tetrahedron (> 1.70 Å). The polyhedral volume of the tetrahedron at one atmospheric pressure is about 4 percent larger than that of forsterite (Smyth and Bish 1988) and therefore may be expected to partition trivalent transition metals from olivine. The O2 position is the bridging oxygen of the Si_2O_7 group and is also bonded to one M2, so it is overbonded. By contrast, O1 is bonded to five Mg, but not to Si, and is thus underbonded. Therefore, the non-silicate O1 is a potential site for protonation and charge balance is commonly maintained by cation vacancy at M3 (Smyth 1987; Jacobsen et al. 2005; Deon et al. 2010; Ye et al. 2010). Protonation in wadsleyite can occur along the O1···O1, O1···O3, O1···O4, O3···O4 edges of a vacant M3 octahedron and the O4···O4 tetrahedral edge of the Si_2O_7 group (Jacobsen et al. 2005; Deon et al. 2010). Gudfinnsson and Wood (1998) determined

the partitioning of Ti, Al, Cr, Ni, Ca, and Na between coexisting olivine and wadsleyite at 1400 to 1600 °C, 13.2 to 14.2 GPa, indicating that all, except Ca, partition preferentially into wadsleyite relative to olivine. The order of preference for wadsleyite is Ni < Na < Cr < Ti < Al, with $D^{wad/ol}$ of about 2 for Ni, 3 for Na, and between 5 and 8 for Cr, Ti, and Al.

Previous experimental studies on iron-bearing wadsleyite have shown that Fe is significantly ordered among the octahedral sites. Under dry conditions, Finger et al. (1993) found that iron strongly avoids M2 and is enriched in both M1 and M3 for wadsleyite samples that were synthesized under various *P-T* conditions (14.5-16.5 GPa and 1400-1800 °C). The same strong ordering of iron was observed by Smyth et al. (2014) in wet and oxidized samples, which were synthesized at lower pressure and temperature (12-14 GPa and 1400 °C), indicating that neither the *P-T* condition nor the incorporation of hydrogen has significant influence on site preferences of iron at octahedral sites in wadsleyite. In addition, Frost and McCammon (2009) reported a 4/3 ratio of Fe^{3+}:Me (Me=Mg^{2+}+Fe^{2+}) and a 8/3 ratio of Fe^{3+}:Si under dry conditions at 12.7-14.5 GPa and 1200-1600 °C. Similar dependencies were observed in hydrous wadsleyites (synthesized at 12-14 GPa and 1400 °C) as well (Bolfan-Casanova et al. 2012; Smyth et al. 2014), implying that the incorporation of hydrogen does not significantly alter the mechanism of Fe^{3+} substitution. Although the ordering of Fe in wadsleyite has been well documented, the reasons for it remain unclear. Fe-Mg wadsleyites are always strongly ordered even when quenched from temperatures above 1400ºC, whereas Fe-Mg olivines rarely show significant cation order. This is true despite the fact that the differences in octahedral site volumes in wadsleyite are smaller than those in olivine. Also, the site preferences for other transition metals in the same period (such as Ti, Cr, V, Co, Ni and Zn) are unknown. In order to better understand cation ordering and transition metal solubilities in wadsleyite, we have synthesized Mg-rich wadsleyites with sufficient amounts of

transition metals, Ti, Cr, V, Co, Ni, and Zn, to observe site preferences by single-crystal X-ray diffraction.

EXPERIMENTAL WORK

Synthesis

Synthesis experiments were conducted in the 1200 tonne Sumitomo multi-anvil press at Bayerisches Geoinstitut, University of Bayreuth, Germany using 14/8 assemblies (14 mm MgO octahedron with 8 mm corner truncations on 32 mm WC cubes and using $LaCrO_3$ heaters). Capsules were 1.6 mm diameter welded Pt with two separate capsules per experiment each 1.4 mm in length. Starting materials were mixed from oxides SiO_2 (quartz), MgO (periclase), $Mg(OH)_2$ (brucite) plus 2 to 3 wt% of either NiO, ZnO, CoO, V_2O_3, Cr_2O_3, or TiO_2 in the six separate capsules. Water (H_2O) content in each experiment was about 1.6 wt% as brucite in the starting material. Heating duration in each experiment was 220 min. Quench to temperatures below 500 °C was about 3 s. Recovered capsules were mounted in epoxy on 24 mm round glass slides and ground to expose the run products.

Electron microprobe analysis

Mineral and melt compositions were determined in all samples using a JEOL 8600 electron microprobe (EPMA) at the University of Colorado, Boulder. Acceleration voltage was 15 kV, beam current was 20 nA, and beam size was 5 µm. Standards for Mg and Si were Fo_{90} olivine, Ni - nickel metal, Co - cobalt metal, Zn - sphalerite, V - vanadium metal, Cr - chromite, and Ti - ilmenite. Water content was estimated using XRD data, and from a relationship between M3 vacancy and hydrogen content derived by Jacobsen et al. 2005. Mineral formula was recalculated assuming a total of four oxygens,

including the estimated water content.

Raman spectroscopy

Raman spectroscopy was conducted at the Raman Microspectroscopy Laboratory at the Department of Geological Sciences, University of Colorado-Boulder. Ambient temperature, unpolarized Raman spectra of all hydrous wadsleyites were collected from randomly oriented specimens with a Horiba LabRam HR Evolution Raman spectrometer with 532 nm laser excitation.

X-ray diffraction

Single wadsleyite crystals were selected from the capsules and mounted on glass fibers for X-ray diffraction analysis. Intensity data were collected on a Bruker APEX II CCD detector on a Siemens/MAC-Science 18 kW rotating Mo-anode X-ray generator at the University of Colorado, Boulder. 50 kV voltage, 250 mA current and calibrated radiation (λ = 0.71073 Å) were used for all measurements. Crystal structure, atom position, occupancy, and displacement parameters were refined from the intensity data sets using SHELXL-97 in package WINGX. For the structure parameter refinement, scattering factors for ionized cations Mg^{2+}, Si^{4+}, Co^{2+}, Ni^{2+}, Zn^{2+}, Cr^{3+} and V^{3+} (Cromer and Mann 1968), and O^{2-} (Tokonami 1965) were used, as these were found to give reliable cation occupancy refinement for pure Mg phases (Smyth et al. 2004; Ye et al. 2009; Smyth et al. 2014). Since the TiO_2 content estimated from sites occupancies on the basis of ionic scattering factor from Cromer and Mann (1968) is inconsistent with microprobe analysis, neutral atom refinement was employed to estimate site preferences of Ti^{4+} in Ti-bearing wadsleyite.

RESULTS AND DISCUSSION

The assemblages of coexisting wadsleyite, clinoenstatite and quench melt in all six capsules are shown in Figs. 2a and 2b. For wadsleyite, the grain size in each sample was approximately 100 μm. Textures typically had wadsleyite in the center with pyroxene in contact with the Pt capsule. The minor transition metals were typically enriched in the wadsleyite relative to the pyroxene imparting strong color to the wadsleyite in the case of Co (red), Ni and Cr (green), and V (yellow-brown), whereas the Ti and Zn wadsleyites remained colorless (see Fig 2a). The focused back-scattered electron images for all six samples are shown in Fig. 2b.

For Co, Ni, V, Cr, and Ti wadsleyites, Raman spectra in the lattice vibration region (0 to 1200 cm^{-1}) show the characteristic wadsleyite structure (see Fig. 3a). Unlike olivine and ringwoodite, wadsleyite is a sorosilicate with Si_2O_7 groups and without individual SiO_4 groups (Smyth 1987). The stretching vibrations of the Si_2O_7 unit can be divided into the symmetric stretch of the disilicate group (Si-O-Si) and the symmetric stretching of the SiO_3 terminal unit (Kleppe et al. 2001 and 2006). Therefore, as shown in Fig.3a, all spectra show the presence of two sharp bands at about 720 cm^{-1} and 920 cm^{-1}, corresponding to the symmetric stretching of Si-O-Si bridges and SiO_3 symmetric stretching, respectively (Kleppe et al. 2001 and 2006). For Co, Ni, and V wadsleyites, the spectra in the 3000 to 3700 cm^{-1} region (see Fig. 3b) displayed broad bands at about 3320 to 3390 cm^{-1}, showing the stretching vibration of OH (Kleppe et al. 2001 and 2006). The spectrum of Zn wadsleyite showed strong fluorescence, thus the lattice vibrations were not observed. Similarly, Ti and Cr wadsleyite samples showed high fluorescence in the > 3000 cm^{-1} range obscuring O-H stretching vibrations (see Fig. 3c).

Detailed electron microprobe chemical analyses of wadsleyites were performed for each of the six samples (see Table 1). The results indicate that wadsleyite can incorporate transition metals Ti, Cr, V, Co, Ni and Zn with significant oxide contents (0.56 %, 3.73 %,

3.40 %, 3.40 %, 5.98 %, and 4.52 % by weight respectively), and the concentrations of these minor transition metals were higher in the wadsleyite than in coexisting pyroxene (0.13 %, 0.46 %, 0.96 %, and 1.86 % by weight for TiO_2, V_2O_3, CoO and ZnO respectively; see Table 2). Since the interference from residual brucite due to size constraint of spot cannot be ruled out, the chemical compositions of quench melt were not reported.

All six synthetic hydrous wadsleyite crystals have been refined by single-crystal X-ray diffraction. The contrast in scattering between the minor transition metals and the major cations (Mg and Si) allows good precision in site occupancy refinements. Crystal structure refinement parameters are summarized in Table 3. Atom position and occupancy are reported in Tables 4, 5, and 6.

Unit cell parameter and vacancy concentration

Jacobsen et al. (2005) reported a systematic study of OH in wadsleyite (synthesized at 16-18 GPa and 1200-2100 °C) and suggested that the substitution of H in wadsleyite gives rise to the expansion of *b* axis and contraction of *a* axis, thus the *b/a* axis length ratio can be used to indicate water content and thus M3 vacancy content if H is charge balanced by M3 vacancy only. Consistent with this hypothesis, Ye et al. (2009) reported more than 20% vacancy at M3 in a hydrous Mg-wadsleyite, which was synthesized at the relatively lower pressure and temperature (12 GPa and 1250 °C). A relationship between vacancy concentration (mainly at M3) and hydrogen content has been derived by Jacobsen et al. (2005) as follows:

$$b/a=2.008+1.25\times10^{-6}\times C_{H2O} \quad (1)$$

where b/a is the length ratio of axes, and C_{H2O} is in ppm H_2O by weight indicating the

water content and thus M3 vacancy concentrations. Calculations of H_2O contents on the basis of equation (1) are shown in Table 1.

Smyth et al. (2014) showed that for Fe-bearing wadsleyites (synthesized at 12-14 GPa and 1400 °C), the Fe contents measured from the single-crystal X-ray refinement based on the vacancy estimation by *b*/*a* ratio are consistent with the Fe contents measured with electron microprobe. Thus, a modified equation put forward by Smyth et al. (2014) on the basis of equation (1) was employed to estimate the M3 vacancies in this study, assuming that number of M3 vacancies per formula unit is equivalent to one half the number of H atoms per formula unit:

$$[\text{vacancy}]=1/2(b/a-2.008)\times Si\times M/11.25 \quad (2)$$

where *Si* and *M* are the number of Si cations per four oxygens and molar mass of the wadsleyite derived from electron microprobe data in Table 1. The estimated M3 vacancies are shown in Table 5.

Co, Ni and Zn incorporation in wadsleyite

Previous experimental studies on high pressure phase transformations of transition metal orthosilicates M_2SiO_4 (M=Mg, Co, Zn, and Ni) indicate that Co, Ni, and Zn can substitute for Mg in the wadsleyite structure. Morimoto et al. (1974) synthesized pure β-Co_2SiO_4 at 1420 °C and 8.1 GPa. Syono et al. (1971) reported the high pressure (13 GPa) synthesis of the spinelloid III phase of Zn_2SiO_4. Although no previous studies support the existence of pure β-Ni_2SiO_4, the spinelloid III phase of Ni-aluminosilicate has been observed as one of the five designated phases (I-V) (Ma 1974; Akaogi et al. 1982),

Consistent with the site preference of Fe in wadsleyite (Finger et al. 1993; Smyth et al. 2014), Ni, Co, and Zn are all strongly ordered avoiding M2 while occupying both M1 and

M3 sites (Fig. 4a). The observed ordering of these divalent cations are not likely to be due to their cation radii alone. For instance, although Ni^{2+} has a smaller ionic radius than Mg^{2+} (Shannon 1976), it shows a similar site preference to the divalent cations (Co^{2+}, Zn^{2+}, and Fe^{2+}) which are larger than Mg^{2+}. Thus, crystal field stabilization energy (CFSE) is considered to be an important factor, which affects the site preferences of these divalent cations.

Effects of crystal field stabilization energy and cation radius on divalent cation ordering

In wadsleyite structure, both the M1 and M2 sites are each bonded to four O4 atoms in a plane normal to *c,* so the four bonds are symmetrically equivalent. Normal to this plane, M1 is bonded to two O3 atoms and the bonds are equivalent and slightly longer than those to the O4 atoms. For M2, however, the bonds normal to the plane of the O4 bonds are very different; the bond to O1 (non-silicate oxygen) is short whereas the bond to O2 (bridging oxygen) is long (see Table 5). According to crystal field theory, the additional splitting of the degenerated electronic ground state of the ion at descending symmetry of the crystal field at M2 must result in lowering of the ground level energy and, thus, in a higher value of CFSE. As shown in Fig. 5a, the estimated CFSE values of Ni^{2+}, Co^{2+}, and Zn^{2+} at octahedral sites in oxide structures (McClure 1957; Dunitz and Orgel 1957; Burns 1993) have a positive correlation with octahedral occupancy ratios (M2/(M1+M3)). Therefore, the site preferences of these divalent cations among three distinct octahedral sites can be explained by the larger negative value of the CFSE, the stronger the stabilizing effect of the transition metal ion in the structure.

In olivine, the octahedral site volumes differences are larger than in wadsleyite with M2 having the larger polyhedral volume. McCarty et al. (2015) reported that Ni^{2+} occupies only M1, Fe^{2+} occupies M1 and M2 roughly equally, and Co^{2+} occupies both

M1 and M2 in an approximately 3:1 ratio, consistent with cation radius and site size, but also revealing a similar positive correlation between calculated CFSE for divalent Ni^{2+}, Co^{2+}, and Fe^{2+} (McClure 1957; Dunitz and Orgel 1957; Burns 1993) (see Fig. 5b). This correlation implies that crystal field effect is an important factor that controls the cation ordering at octahedral sites in both wadsleyite and olivine.

As shown in Figs. 4a and 5a, Zn shows a weak site preference among octahedral sites in wadsleyite, though Zn^{2+} has 10 electrons in *d*-orbitals and hence no CFSE. This phenomenon is possibly related to the anisotropic length change in axes. According to Finger et al. (1993), the elongations of the *a* and *c* axes due to Fe^{2+} substitution are inconsistent with that of *b*, and this anisotropy results in the relative depletion of Fe^{2+} in M2 relative to M1 and M3. Also, the inconsistent elongations of the axes can possibly restrict the solubility of Zn^{2+} in M2 octahedron, since Zn^{2+} has larger ionic radius than Mg^{2+} (Shannon 1976).

For ionic radii, divalent Fe^{2+}, Zn^{2+}, Co^{2+}, and Ni^{2+} are much larger than trivalent Fe^{3+}, V^{3+}, and Cr^{3+} (Shannon 1976), and they are too large to substitute into tetrahedral sites in wadsleyite. This prediction was verified by the calculated occupancy radios (2T/(M1+M2+2M3)), which reveal the proportion of transition metal ions at tetrahedral sites (see Fig. 6). Similarly, the comparatively high occupancy of Ni^{2+} (see Table 5 and Fig. 4a) at M1 can also be attributed to the effects of cation radius and octahedral volume. Unlike Co^{2+} and Zn^{2+}, Ni^{2+} is smaller than Mg^{2+} (Shannon 1976), thus it is more likely to occupy M1, which has a slightly smaller octahedral volume than M3.

For divalent cations, Co^{2+} has a larger negative CFSE value than Fe^{2+} (McClure 1957; Dunitz and Orgel 1957; Burns 1993), whereas the occupancy ratio (M2/(M1+M3)) of Fe^{2+} in dry system (see Table 2 of Finger et al. 1993) is less than that of Co^{2+} under

hydrous conditions (see Table 5 and Fig 5a). This disagreement is possibly related to H substitution and the size of the ferrous cation. Although hydrogen is not likely to affect the site preferences of divalent cations at octahedral sites in wadsleyite (Finger et al. 1993; Smyth et al. 2014), H substituting into octahedral sites ($Mg^{2+} = 2H^{+}$; Inoue et al. 1995) can lower the occupancy of Co^{2+} at M3, and thus may result in a relatively higher occupancy ratio (M2/(M1+M3)), since vacancies at octahedral sites mainly occur at M3 (Jacobsen et al. 2005). In addition, Hazen et al. (2000a) cited some evidences for M2 being the smallest octahedron in Fe-bearing wadsleyite under high pressure (over 8 GPa). Thus, for Fe^{2+}, it is more difficult to substitute into the smaller M2 because of its large ionic radius (larger than Mg^{2+} according to Shannon 1976).

Cr and V incorporation in wadsleyite

In agreement with previous experimental studies on incorporation of trivalent cations in wadsleyite (Gudfinnsson and Wood 1998; O'Neill et al. 1996; Woodland and Angel 1998; Deon et al. 2011; Smyth et al. 2014), our microprobe analyses demonstrate that significant amounts of Cr_2O_3 (3.73 wt%) and V_2O_3 (3.40 wt%) can substitute into wadsleyite (see Table 1). X-ray structure refinements in this study show that Cr and V have a strong preference for M3 over M1 and M2 and significant substitution up to 3.4 % (atomic percent) at the M3 site (see Fig. 4b and Table 5). For T site, 2.7 % and 2.1 % can be occupied by V and Cr respectively (see Fig. 4b and Table 6).

The substitution of trivalent Cr^{3+} and V^{3+} can be explained by the following equation, which is modified from Bolfan-Casanova et al. (2012) and Smyth et al. (2014) previously reported equations of Fe^{3+} substitution in Fe-bearing wadsleyites:

$$6(OH)_O^{\cdot}+3V_{Me}^{''}+4Tr_2O_3+6Mg_{Me}^{x}+2Si_{Si}^{x} = 6Tr_{Me}^{\cdot}+3V_{Me}^{''}+2Tr_{Si}^{'}+2(OH)_O^{\cdot}+6MgO$$
$$+2SiO_2+2H_2O+2O_O^{x}+O_2 \quad (3)$$

In equation (3), V is vacancy, Tr is trivalent cation (Cr^{3+} or V^{3+}), in Kröger-Vink notation (Kröger and Vink 1956) the subscripts refer to the site (Me for octahedral site, Si for tetrahedral site and O for oxygen position), and the superscripts to the charge ([·] for an excess positive charge, ['] for an excess negative charge and x for charge neutrality). The trivalent Cr^{3+} and V^{3+} in the tetrahedral site and the hydroxyl defects can associate to form neutral defect complexes:

$$Tr_{Si}^{'}+(OH)_{O}^{\cdot} = (TrH)_{Si}^{x}+O_{O}^{x} \quad (4)$$

As shown in equation (3), the incorporation of Cr^{3+} and V^{3+} is corresponding to the formation of octahedral vacancies. Since these vacancies mainly occur at M3 (Jacobsen et al. 2005), Cr and V are more likely to occupy M3 site comparing with M1 and M2 (see Fig. 4b).

Trivalent cations in the tetrahedral site

The calculated occupancy ratios (2T/(M1+M2+2M3)) of Cr and V are much higher than those of Ni and Co (see Fig. 6), implying that Cr and V tend to occupy both octahedral and tetrahedral sites. Although the possible presence of minor Cr^{6+} and V^{5+} cannot be ruled out, the higher-than-expected occupancies of Cr and V at the tetrahedral sites are possibly due to the specialty of wadsleyite structure.

The tetrahedral volume in wadsleyite is larger than that in olivine (Smyth and Bish 1988). Therefore wadsleyite is predicted to incorporate more Cr^{3+} and V^{3+} (larger than Si^{4+} according to Shannon 1976) in its tetrahedral site. According to Smyth et al. (2014), trivalent cations in the tetrahedron are predicted to stabilize the wadsleyite structure by increasing the overall size of the site, especially the distances to the non-bridging

oxygens. In addition, trivalent cations substituting into this site can reduce the site potential at O2, relieve the overbonding of the bridging oxygen, and decrease the distortion (Woodland and Angel 1998; Smyth et al. 2014). Therefore both Cr and V have relatively high occupancies at the tetrahedral sites.

Partition of Cr and V around wadsleyite-olivine boundary

As shown in Fig. 7a, the solubility of Cr in olivine (Gudfinnsson and Wood 1998) is significantly lower than that in wadsleyite. Also, Price et al. (1983) demonstrated that natural wadsleyite has greater capability of incorporating Cr comparing with coexisting olivine from Peace River meteorite (see Fig. 7b). Since V and Cr have similar ionic radii (Shannon 1976) and nearly identical mechanism of substitution, in all probability, wadsleyite is more likely than coexisting olivine to incorporate V as well. Therefore, Cr and V may be enriched in a melt or an accessory phase if hydrous melting occurs on upward convection across the wadsleyite-olivine boundary.

Ti incorporation in wadsleyite

The solubilities of TiO_2 in both wadsleyite (0.56 wt%; see Table 1) and coexisting pyroxene (0.13 wt%; see Table 2) are relatively low compared to Cr_2O_3, V_2O_3, ZnO, NiO and CoO. This preference is in agreement with Mibe et al. (2006) previous reported element partitioning between transition-zone minerals and melt (Ti prefers melt to wadsleyite) under hydrous conditions.

For tetravalent Ti^{4+}, the site preferences $Ti_{M3}>Ti_{M1}>Ti_{M2}\approx Ti_T$ (see Fig. 4c, Tables 5 and 6) have been recorded on the basis of X-ray structure refinement results. From *b/a* axial length ratios, we estimate 4.8 % (atomic percent) M3 vacancies (see Table 5). The inferred substitution mechanism of Ti^{4+} is shown below.

$$TiO_2+2Mg_{Me}^{x}=Ti_{Me}^{\cdot\cdot}+V_{Me}^{''}+2MgO \qquad (5)$$

The incorporation of Ti^{4+} in wadsleyite also results in formation of octahedral vacancies. Since these vacancies are mainly at M3 (Jacobsen et al. 2005), the site occupancy of Ti^{4+} at M3 is apparently greater than M1 and M2 as shown in Fig. 4c.

The direct substitution of Ti^{4+} on the T site can be written in the following reaction.

$$TiO_2+Si_{Si}^{x}=Ti_{Si}^{x}+SiO_2 \quad (6)$$

According to Inoue et al. (1995) and Bolfan-Casanova et al. (2012), the incorporation mechanism of H^+ can be interpreted as below.

$$H_2O+2O_O^{x}+Mg_{Me}^{x}=V_{Me}''+2(OH)_O^{\cdot}+MgO \quad (7)$$

with formation of defect associates:

$$V_{Me}''+2(OH)_O^{\cdot}=(2H)_{Me}^{x} \quad (8)$$

Ti partition around wadsleyite-olivine boundary

Dobrzhinetskaya et al. (2000a) analyzed the conditions that were responsible for the high solubility of TiO_2 in olivine, and conclude that it must be involved with extremely high pressure (12 GPa for 1 wt%). They conducted experiments with multi-anvil apparatus under various *P-T* conditions and showed a positive correlation between

pressure and solubility of TiO_2, indicating that olivine has a greater ability to incorporate TiO_2 near olivine-wadsleyite boundary than in upper mantle, especially at higher temperatures. Consistent with Gudfinnsson and Wood (1998) previous reported partitioning of Ti between wadsleyite and olivine, our microprobe analysis shows that wadsleyite has relatively greater capability of incorporating TiO_2 comparing with olivine (see Fig. 7a). Therefore, if hydrous melting occurs on upward convection across the wadsleyite-olivine boundary, Ti is likely to partition into melt or other accessory phases, and be depleted in olivine with upwelling.

IMPLICATIONS

First, X-ray structure refinement results show that Ni, Co, and Zn substitute up to 7 % (atomic percent) at octahedral sites. They are all strongly ordered avoiding M2 while enriched in both M1 and M3 sites, and the occupancies in tetrahedral sites are lower than those in all three octahedral sites. Cr and V show the preferences for M3 and T over M1 and M2 sites. Ti tends to substitute into M3 octahedron, and the site occupancy is significantly greater than that at M1, M2 and T sites.

Second, for Ni, Co, and Zn, the observed cation orderings are inconsistent with their divalent cation radii, although the relatively low occupancies at tetrahedral sites and the relatively high occupancy of Ni at M1 are possibly related to cation radii and site sizes. The avoidance of Ni, Co, and Fe for the M2 site in both wadsleyite and olivine can be partially controlled by crystal field stabilization energy (CFSE). The estimated CFSE values of Ni^{2+}, Co^{2+}, Zn^{2+}, and Fe^{2+} (McClure 1957; Dunitz and Orgel 1957; Burns 1993) show a positive correlation with occupany ratios (M2/(M1+M3)) of these transition metals, indicating the larger negative value of the CFSE, the stronger the stabilizing effect of the transition metal ion in the structure.

Third, our experiments reveal that Cr, V and Ti have greater solubilities in wadsleyite

than in olivine. If whole-mantle convection has taken place, much of the bulk silicate Earth has been through this phase and may have fractionated against melt at 410 km depth (Bercovici and Karato 2003). Therefore our experiments indicate that Ti, Cr and V may be enriched in a melt or an accessory phase if hydrous melting occurs on upward convection across the wadsleyite-olivine boundary.

ACKNOWLEDGEMENTS

This study was supported by U.S. National Science Foundation Grant EAR 11-13369 and EAR 14-16979 to JRS. SDJ acknowledges support from NSF EAR-1452344, the Carnegie/DOE Alliance Center, the David and Lucile Packard Foundation, and the Alexander von Humboldt Foundation. Multianvil experiments were supported by Bayerisches Geoinstitut Visitors Program. Raman spectroscopy was conducted at the Raman Microspectroscopy Laboratory at the Department of Geological Sciences, University of Colorado-Boulder, and we gratefully acknowledge the assistance of Mr. Eric Ellison.

REFERENCES

Akaogi, M., Akimoto S., Horioka, H., Takahashi, K., and Horiuchi, H. (1982) The system $NiAl_2O_4$-Ni_2SiO_4 at high pressures and high temperatures: spinelloids with spinel-related structures. Journal of Solid State Chemistry, 44, 257-267.

Bercovici, D., and Karato, S.-I. (2003) Whole-mantle convection and the transition-zone water filter. Nature, 425, 39-44.

Bolfan-Casanova, N., Keppler, H., and Rubie, D. (2000) Water partitioning between nominally anhydrous minerals in the $MgO–SiO_2–H_2O$ system up to 24 GPa: implications for the distribution of water in the earth's mantle. Earth and Planetary Science Letters, 182, 209–221.

Bolfan-Casanova, N., Munoz, M., McCammon, C., Deloule, E., Ferot, A., Demouchy, S.,

France, L., Andrault, D., and Pascarelli, S. (2012) Ferric iron and water incorporation in wadsleyite under hydrous and oxidizing conditions: a XANES, Mössbauer, and SIMS study. American Mineralogist, 97(8-9), 1483-1493.

Burns, R.G. (1993) Mineralogical Applications of Crystal Field Theory, 2nd ed. Cambridge University Press, Cambridge, 551 pp.

Cromer, D.T., and Mann, J. (1968) X-ray scattering factors computed from numerical Hartree-Fock wave functions. Acta Crystallographica, A24, 321-325.

Demouchy, S., Deloule, E., Frost, D.J., and Keppler, H. (2005) Pressure and temperature dependence of water solubility in Fe-free wadsleyite. American Mineralogist, 90, 1084-1091.

Deon, F., Koch-Müller, M., Rhede, D., Gottschalk, M., Wirth, R., and Thomas, S.-M. (2010) Location and quantification of hydroxyl in wadsleyite: New insights. American Mineralogist, 95, 312-322.

Deon, F., Koch-Müller, M., Rhede, D., and Wirth, R. (2011) Water and Iron effect on the P-T-x coordinates of the 410-km discontinuity in the Earth upper mantle. Contributions to Mineralogy and Petrology, 161, 4, 653-666.

Dobrzhinetskaya, L., Bozhilov, K.N., and Green, H.W. II. (2000a) The solubility of TiO_2 in olivine: implications for the mantle wedge environment. Chemical Geology, 163, 325–338.

Dunitz, J.D., and Orgel, L.E. (1957) Electronic properties of transition element oxides. II. Cation distribution amongst octahedral and tetrahedral sites. Journal of Physics and Chemistry of Solids, 3, 318-33.

Finger, L.W., Hazen, R.M., Zhang, J., Ko, J., and Navrotsky, A. (1993) The effect of Fe on the crystal structure of wadsleyite β-$(Mg_{1-x}Fe_x)SiO_4$, $0.00 \leq x \leq 0.40$. Physics and Chemistry of Minerals, 19, 361–368.

Frost, D.J., and McCammon, C.A. (2009) The effect of oxygen fugacity on the olivine to wadsleyite transformation: Implications for remote sensing of mantle redox state at the 410 km seismic discontinuity. American Mineralogist, 94, 872-882.

Gudfinnsson, G.H., and Wood, B.J. (1998) The effect of trace elements on the olivine-wadsleyite transformation. American Mineralogist, 83, 1037-1044.

Hazen, R.M., Weinberger, M.B., Yang, H., and Prewitt, C.T. (2000a) Comparative high-pressure crystal chemistry of wadsleyite, -$(Mg_{1-x}Fe_x)_2SiO_4$, with x = 0 and 0.25. American Mineralogist, 85, 770-777.

Inoue, T., Yurimoto, H., and Kudoh, Y. (1995) Hydrous modified spinel, $Mg_{1.75}SiH_{0.5}O_4$: a new reservoir in the mantle transition region. Geophysical Research Letters, 22, 117-120.

Inoue, T., Wada, T., Sasaki, R., and Yurimoto, H. (2010) Water partitioning in the Earth's mantle. Physics of the Earth and Planetary Interiors, 183, 245–251.

Jacobsen, S.D., Demouchy, S., Frost, D.J., Boffa-Ballaran, and T., Kung, J. (2005) A systematic study of OH in hydrous wadsleyite from polarized FTIR spectroscopy and single-crystal X-ray diffraction: Oxygen sites for hydrogen storage in the Earth's interior. American Mineralogist, 90, 61-70.

Kawamoto, T., Hervig, R.H., and Holloway, J.R. (1996) Experimental evidence for a hydrous transition zone in the early Earth's mantle. Earth and Planetary Science Letters, 142, 587–592.

Kleppe, A.K., Jephcoat, A.P., Olijnyk, H., Slesinger, A.E., Kohn, S.C., and Wood, B.J. (2001) Raman spectroscopic study of hydrous wadsleyite (β-Mg_2SiO_4) to 50 GPa. Physics and Chemistry of Minerals, 28(4), 232–241.

Kleppe, A.K., Jephcoat, A.P., and Smyth, J.R. (2006) High-pressure Raman spectroscopic study of Fo_{90} hydrous wadsleyite. Physics and Chemistry of Minerals, 32(10),

700–709.

Kohlstedt, D.L., Keppler, H., and Rubie, D.C. (1996) Solubility of water in the α, β, and γ phases of $(Mg, Fe)_2SiO_4$. Contributions to Mineralogy and Petrology, 123, 345–357.

Kröger, F.A., and Vink, H.J. (1956) Relationship between the concentration of imperfections in crystalline solids. Solid state physics, Volume 3, p. 307 Academic Press, New York.

Ma, C.B. (1974) New orthorhombic phases on the join $NiAl_2O_4$ (spinel analog)-Ni_2SiO_4 (olivine analog): stability and implications to mantle mineralogy. Contributions to Mineralogy and Petrology, 45, 257–279.

McCarty, R.J., Palke, A.C., Stebbins, J.F., and Hartman, J.S. (2015) Transition metal cation site preferences in forsterite (Mg_2SiO_4) determined from paramagnetically shifted NMR resonances. American Mineralogist, 100, 1265-1276.

McClure, D.S. (1957) The distribution of transition metal cations in spinels. Journal of Physics and Chemistry of Solids, 3, 311-17.

Mibe, K., Orihashi, Y., Nakai, S., and Fujii, T. (2006) Element partitioning between transitionzone minerals and ultramafic melt under hydrous conditions. Geophysical Research Letters, 33, L16307.

Morimoto, N., Tokonami, M., Watanabe, M., and Koto, K. (1974) Crystal Structures of Three Polymorphs of Co_2SiO_4. American Mineralogist, 59, 475-485.

O'Neill, H.S.C., Rubie, D.C., Canil, D., Geiger, C.A., Ross, I.C.R., Seifert, F., and Woodland, A. (1996) Ferric iron in the upper mantle and in transition zone assemblages: implications for relative oxygen fugacities in the mantle. Evolution of the Earth and Planets, Washington, DC, AGU Monograph 74.

Price, G.D., Putnis, A., Agrell, S.O., and Smith, D.G.W. (1983) Wadsleyite, natural $(Mg, Fe)_2SiO_4$ from the peace river meteorite. Canadian Mineralogist, 21, 29-35.

Shannon, R.D. (1976) Revised effective ionic radii and systematic studies of interatomic distances in halides and chalcogenides. Acta Crystallographica, A32, 751-767.

Smyth, J.R. (1987) β-Mg_2SiO_4: a potential host for water in the mantle? American Mineralogist, 72, 1051-1055.

Smyth, J.R., and Bish, D.L. (1988) Crystal structures and cation sites of the rock-forming minerals. Allen and Unwin, Boston.

Smyth, J.R., Kawamoto, T., Jacobsen, S.D., Swope, R.J., Herving, R.L., and Holloway, J.R. (1997) Crystal structure of monoclinic hydrous wadsleyite. American Mineralogist, 82, 270-275.

Smyth, J.R., Holl, C.M., Frost, D.J., and Jacobsen, S.D. (2004) High pressure crystal chemistry of hydrous ringwoodite and water in the Earth's interior. Physics of the Earth and Planetary Interiors, 143-144, 271-278.

Smyth, J.R., Bolfan-Casanova, N., Avignant, D., El-Ghozzi, M., and Hirner, S.M. (2014) Tetrahedral ferric iron in oxidized hydrous wadsleyite, American Mineralogist, 99, 458-466.

Syono, Y., Akimoto, S., and Matsui, Y. (1971) High pressure transformations in zinc silicates. Journal of Solid State Chemistry, 3, 369-380.

Tokonami, M. (1965) Atomic scattering factor for O^{2-}. Acta Crystallographica, 19, 486.

Woodland, A.B., and Angel, R.J. (1998) Crystal structure of a new spinelloid with the wadsleyite structure in the system Fe_2SiO_4-Fe_3O_4 and implications for the Earth's mantle. American Mineralogist, 83, 404-408.

Ye, Y., Schwering, R.A., and Smyth, J.R. (2009) Effects of hydration on thermal expansion of forsterite, wadsleyite, and ringwoodite at ambient pressure. American Mineralogist, 94, 899-904.

Ye, Y., Smyth, J.R., Hushur, A., Manghnani, M.H., Lonappan, D., Dera, P., and Frost, D.J. (2010) Crystal structure of hydrous wadsleyite with 2.8% H_2O and compressibility to 60 GPa. American Mineralogist, 95, 1765-1772.

FIGURE CAPTIONS

Figure 1. Polyhedral representation of the wadsleyite structure (*c* is vertical, *b* is horizontal). O2 is the bridging oxygen of the Si_2O_7 group and is also bonded to one M2. O1 is bonded to five Mg, but not to Si.

Figure 2 a. Scanning electron microscope images and **b.** Back-scattered electron images of coexisting wadsleyite, clinoenstatite and quench melt in all six capsules. Abbreviation: Wd = wadsleyite and Px = clinoenstatite.

Figure 3. Raman spectra of Co, Cr, Ni, Ti, and V wadsleyites in the frequency range (a) 0 to 1200 cm^{-1} showing the features due to the Si_2O_7 (Si-O-Si) symmetric stretching (at about 720 cm^{-1}) and SiO_3 symmetric stretching vibrations (at about 920 cm^{-1}); (b) and (c) 3000 to 3700 cm^{-1}, showing the features due to O-H stretching. The Raman spectrum of Zn wadsleyite is difficult to interpret because of extreme background fluorescence interference and the limitation of signal / noise ratio.

Figure 4. Occupanices of transition metal cations at M1, M2, M3, and T sites. (a) Ni, Co, and Zn; (b) V and Cr; (c) Ti. For Ni, Co, Zn, V and Cr, sattering factors from Cromer and Mann (1968) are used to estimate occupancies while Ti occupancies is determined by neutral atom refinement.

Figure 5 a. The positive correlation between occupancies ratios (M2/(M1+M3)) and the

estimated crystal field stabilization energy (McClure 1957; Dunitz and Orgel 1957; Burns 1993) of divalent cations in octahedron for Ni^{2+}, Co^{2+}, and Zn^{2+} in wadsleyite. **b.** the positive correlation between reported occupancies ratios (M2/M1; McCarty et al. 2015) and the estimated crystal field stabilization energy of divalent cations in octahedron for Ni^{2+}, Co^{2+} and Fe^{2+} in olivine.

Figure 6. Occupancy ratios (2T/(M1+M2+2M3)) of transition metal cations Ni^{2+}, Co^{2+}, Zn^{2+}, Fe^{2+}, Fe^{3+}, Cr^{3+}, and V^{3+} in wadsleyite (for Cr and V, possible presence of minor Cr^{6+} and V^{5+} cannot be ruled out). T is tetrahedral site; M1, M2, and M3 are three symmetrically distinct octahedral sites.

Figure 7 a. Concentrations of transition metals Ti, Cr, V, Ni, Co and Zn in wadsleyites from this study and the maximum observed solubilities of transition metal oxides NiO, TiO_2, Cr_2O_3 and Al_2O_3 in wadsleyite and olivine reported by Gudfinnsson and Wood (1998) (experiments were conducted at 1400 to 1600 °C, 13.2 to 14.2 GPa, starting mixtures are sintered olivine compositions containing either 0 or 1 wt% NiO, Cr_2O_3, Al_2O_3, or TiO_2, arrows indicate that saturation with Ni was not seen, and the solubility is limited only by the amount of trace element they present). **b.** the maximum observed solubilities of transition metals Zn, Ni,and Cr in natural wadsleyites and olivine in fragments from Peace River meteorite (Price et al. 1983).

Figure 1

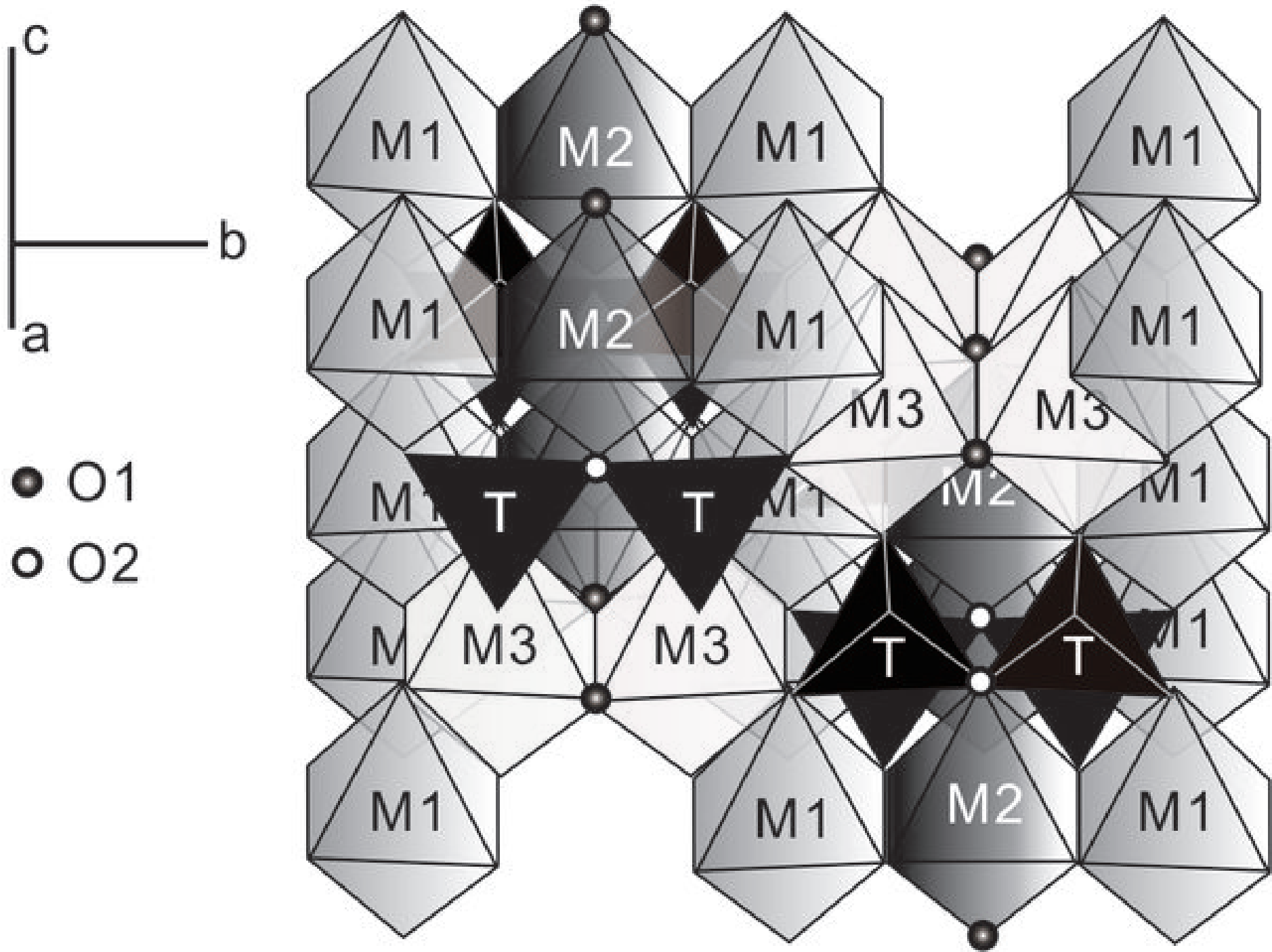

Figure 2

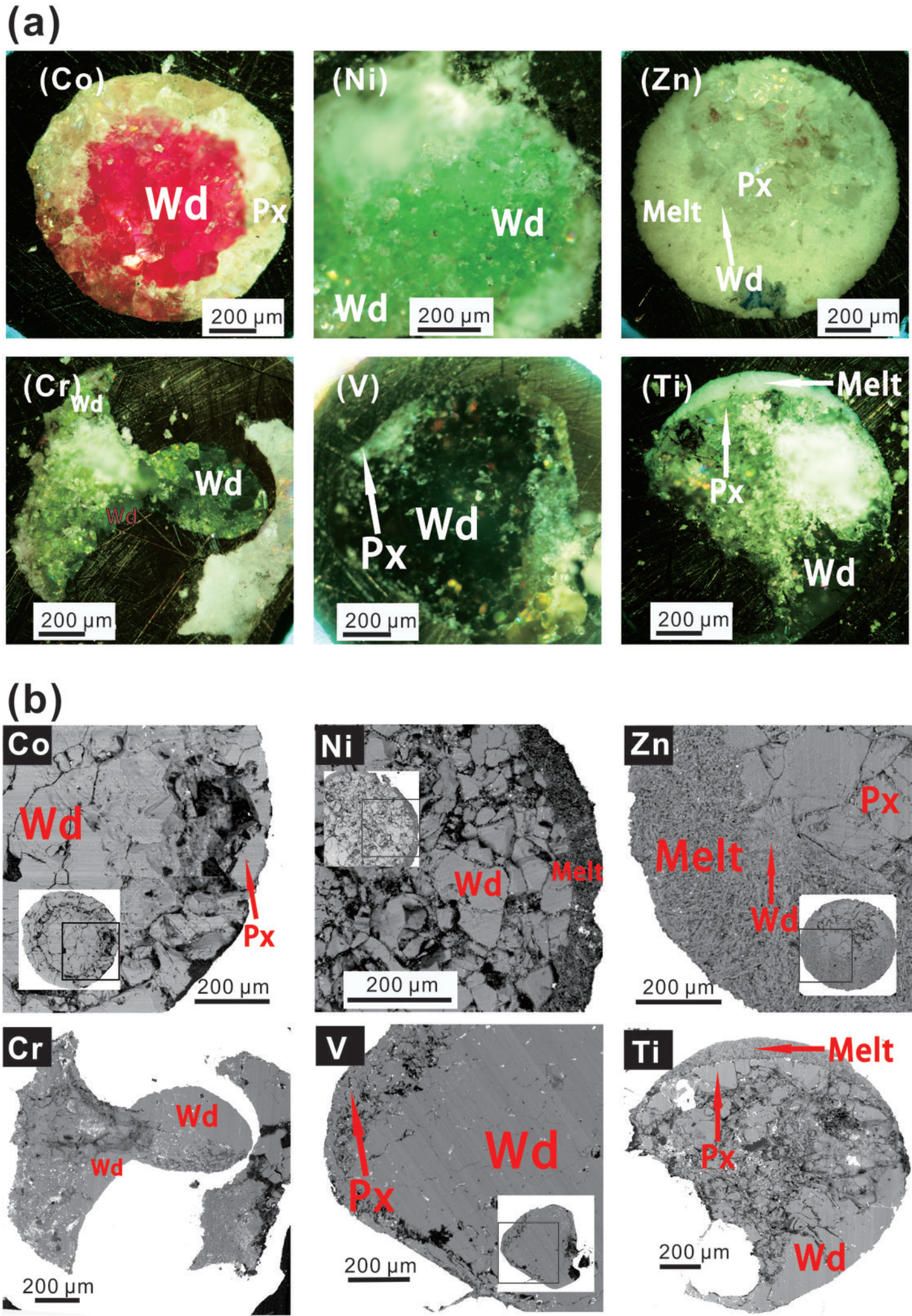
(a)
(Co)
Wd
Px
200 µm
(Ni)
Wd
Wd
200 µm
(Zn)
Px
Melt
Wd
200 µm
(Cr)
Wd
Wd
Wd
200 µm
(V)
Wd
Px
200 µm
(Ti)
Melt
Px
Wd
200 µm
(b)
Co
Wd
Px
200 µm
Ni
Wd
Melt
200 µm
Zn
Px
Melt
Wd
200 µm
Cr
Wd
Wd
200 µm
V
Wd
Px
200 µm
Ti
Melt
Px
Wd
200 µm

Figure 3

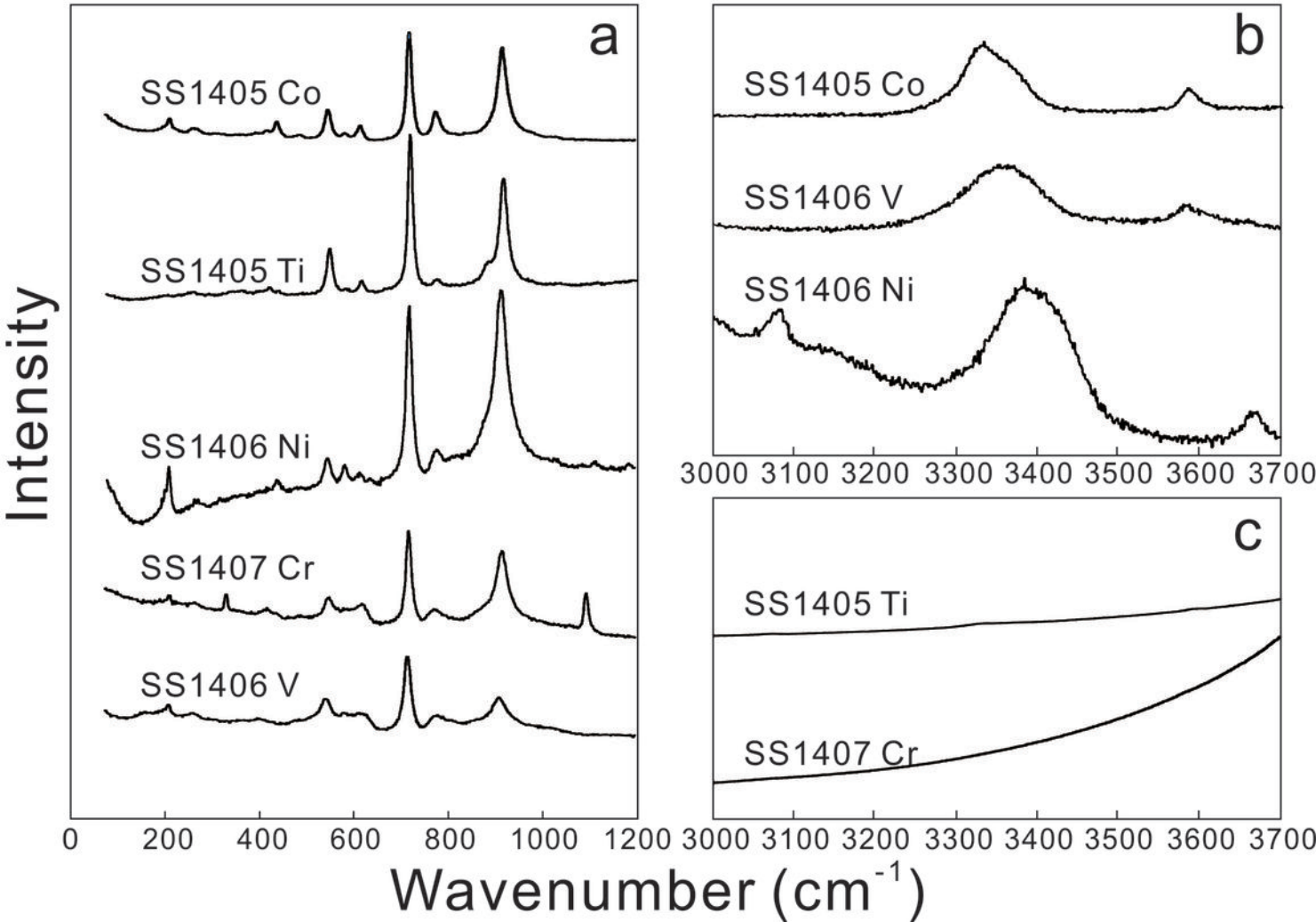
a
SS1405 Co
SS1405 Ti
SS1406 Ni
SS1407 Cr
SS1406 V
b
SS1405 Co
SS1406 V
SS1406 Ni
c
SS1405 Ti
SS1407 Cr
Intensity
0 200 400 600 800 1000 1200
3000 3100 3200 3300 3400 3500 3600 3700
3000 3100 3200 3300 3400 3500 3600 3700
Wavenumber (cm^{-1})

Figure 4

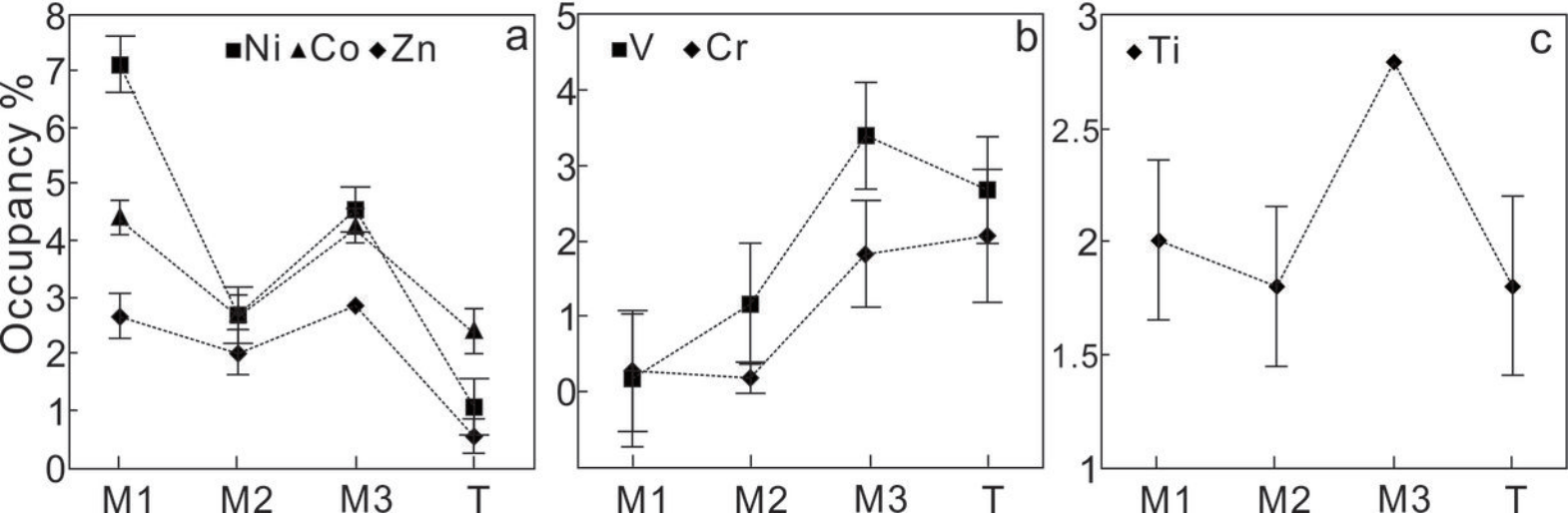

Figure 5

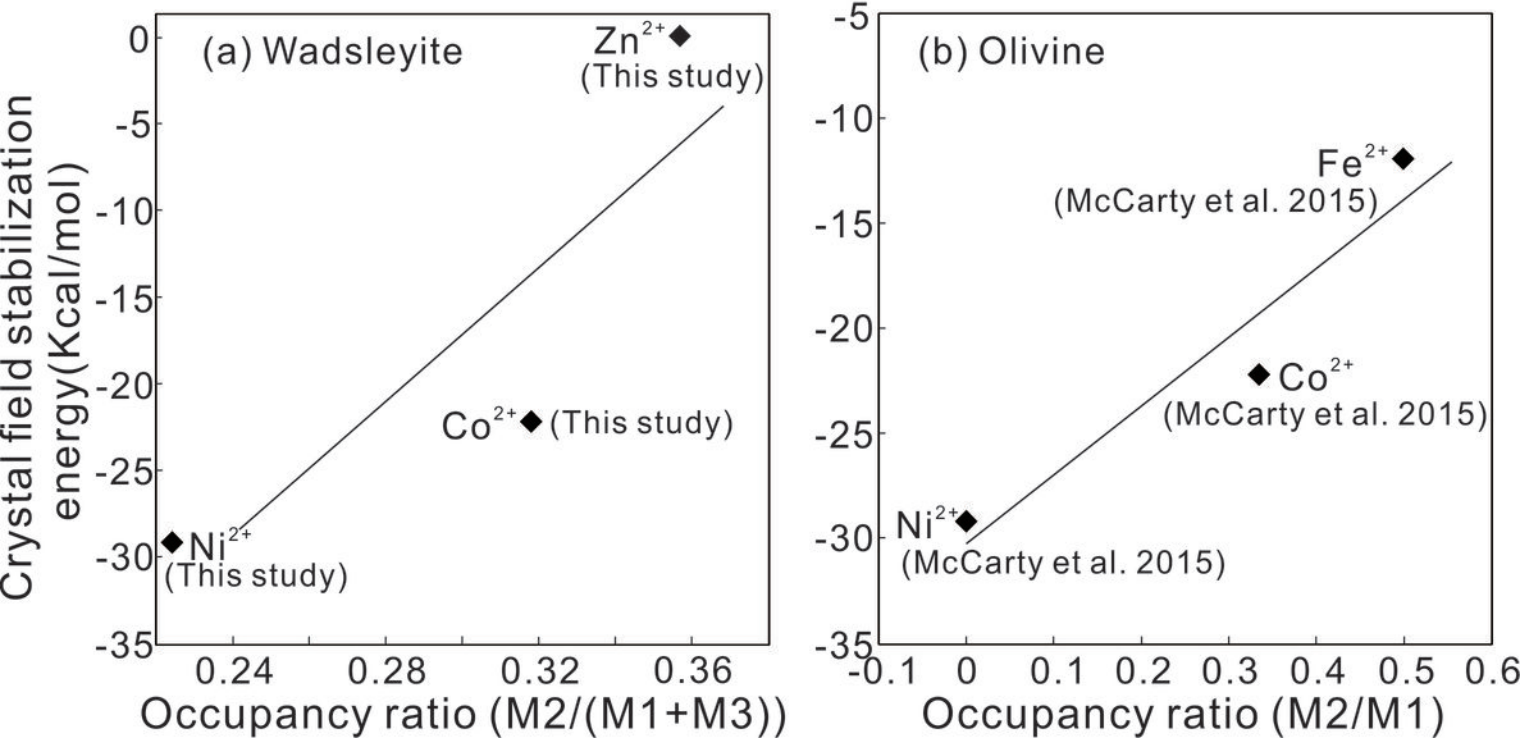
(a) Wadsleyite
Zn2+
(This study)
Co2+ (This study)
Ni2+
(This study)
Crystal field stabilization energy(Kcal/mol)
0
-5
-10
-15
-20
-25
-30
-35
0.24
0.28
0.32
0.36
Occupancy ratio (M2/(M1+M3))
(b) Olivine
Fe2+
(McCarty et al. 2015)
Co2+
(McCarty et al. 2015)
Ni2+
(McCarty et al. 2015)
-5
-10
-15
-20
-25
-30
-35
-0.1
0
0.1
0.2
0.3
0.4
0.5
0.6
Occupancy ratio (M2/M1)

Figure 6

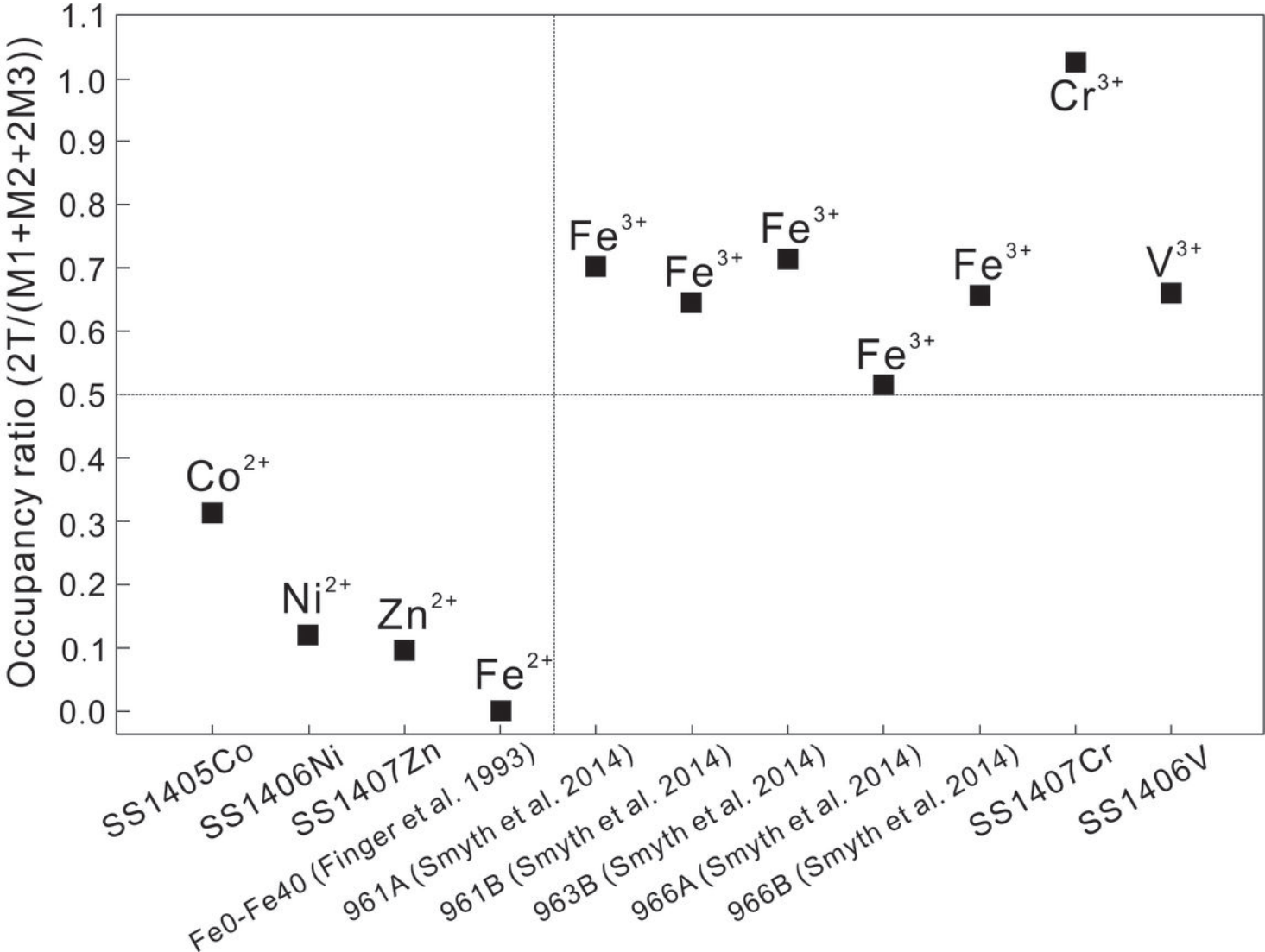
Occupancy ratio (2T/(M1+M2+2M3))
1.1
1.0
0.9
0.8
0.7
0.6
0.5
0.4
0.3
0.2
0.1
0.0
Co2+
Ni2+
Zn2+
Fe2+
Fe3+
Fe3+
Fe3+
Fe3+
Fe3+
Cr3+
V3+
SS1405Co
SS1406Ni
SS1407Zn
Fe0-Fe40 (Finger et al. 1993)
961A (Smyth et al. 2014)
961B (Smyth et al. 2014)
963B (Smyth et al. 2014)
966A (Smyth et al. 2014)
966B (Smyth et al. 2014)
SS1407Cr
SS1406V

Figure 7

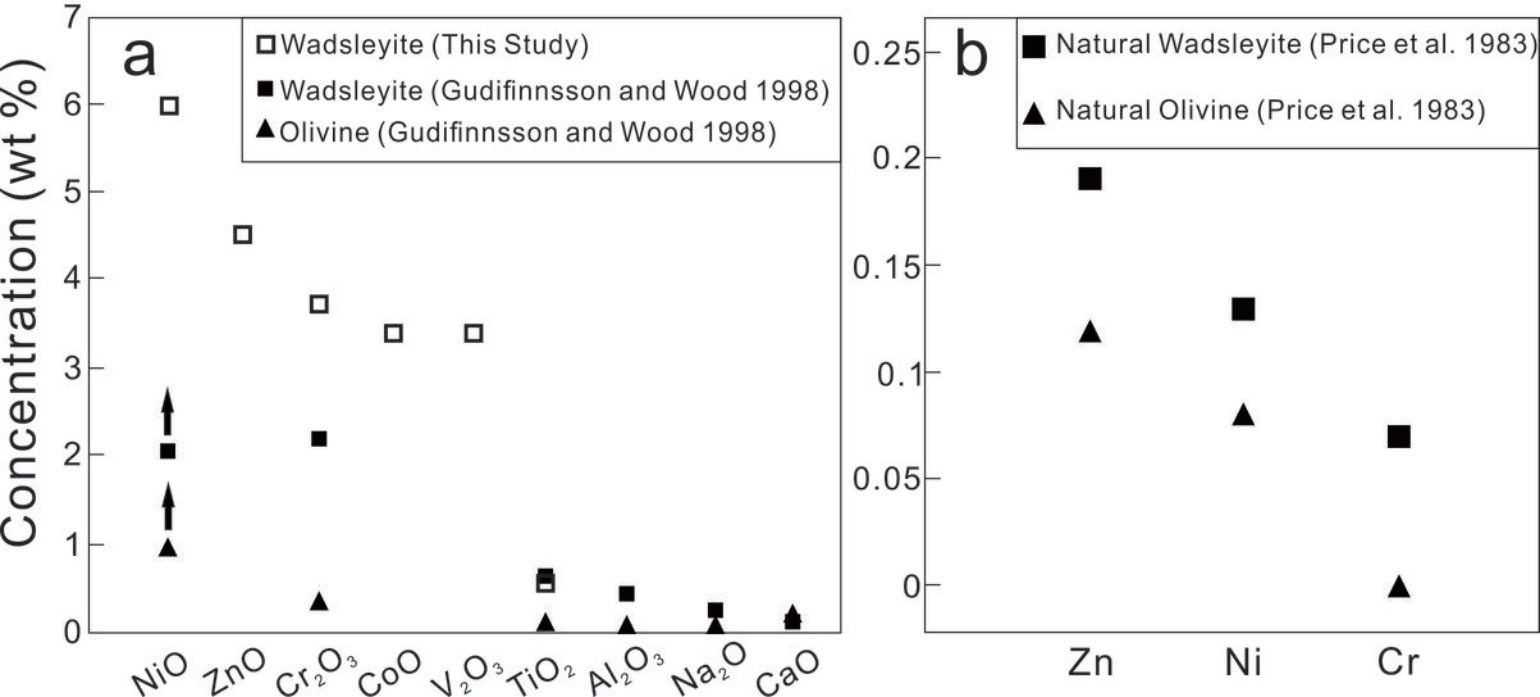
a
Wadsleyite (This Study)
Wadsleyite (Gudifinnsson and Wood 1998)
Olivine (Gudifinnsson and Wood 1998)
Concentration (wt %)
0
1
2
3
4
5
6
7
NiO
ZnO
Cr_2O_3
CoO
V_2O_3
TiO_2
Al_2O_3
Na_2O
CaO
b
Natural Wadsleyite (Price et al. 1983)
Natural Olivine (Price et al. 1983)
0
0.05
0.1
0.15
0.2
0.25
Zn
Ni
Cr

Table1. Electron microprobe chemical analyses for six wadsleyites.

Oxide (wt%)	SS1405Co	SS1406Ni	SS1406V	SS1407Cr	SS1407Zn	SS1407Ti
SiO_2	41.90	39.80	43.10	42.85	42.17	42.77
TiO_2	0.00	0.00	0.00	0.00	0.00	0.56
Cr_2O_3	0.00	0.00	0.00	3.73	0.00	0.00
V_2O_3	0.00	0.00	3.40	0.00	0.00	0.00
MgO	53.05	50.73	50.67	52.64	52.78	55.34
CoO	3.40	0.00	0.00	0.00	0.00	0.00
NiO	0.00	5.98	0.00	0.00	0.00	0.00
ZnO	0.00	0.00	0.00	0.00	4.52	0.00
H_2O[a]	0.98	1.61	2.69	1.14	0.46	0.62
Total	99.33	98.12	99.86	100.36	99.93	99.29
Cations per 4 Oxygens						
Si	0.99	0.96	0.99	0.99	1.00	1.00
Ti	0.00	0.00	0.00	0.00	0.00	0.01
Cr	0.00	0.00	0.00	0.07	0.00	0.00
V	0.00	0.00	0.06	0.00	0.00	0.00
Mg	1.87	1.83	1.73	1.82	1.87	1.93
Co	0.06	0.00	0.00	0.00	0.00	0.00
Ni	0.00	0.12	0.00	0.00	0.00	0.00
Zn	0.00	0.00	0.00	0.00	0.08	0.00
H	0.15	0.26	0.41	0.18	0.07	0.10
Total	3.08	3.17	3.19	3.06	3.03	3.03
Wads Molar Mass	141.303	142.520	137.247	139.855	142.596	139.343

[a]all water contents estimated by equation: $b/a=2.008+1.25\times10^{-6}\times C_{H2O}$, see Jacobsen et al. (2005)

Table 2. Electron microprobe chemical analyses for four pyroxenes.

Oxide (wt%)	SS1405Co	SS1406V	SS1407Zn	SS1407Ti
SiO_2	50.99	50.76	53.27	53.15
TiO_2	0.00	0.00	0.00	0.13
V_2O_3	0.00	0.46	0.00	0.00
MgO	40.71	40.76	39.40	41.65
CoO	0.96	0.00	0.00	0.00
ZnO	0.00	0.00	1.86	0.00
Total	92.66	91.98	94.53	94.93
Cations per 4 Oxygens				
Si	1.25	1.25	1.28	1.26
Ti	0.00	0.00	0.00	0.00
V	0.00	0.01	0.00	0.00
Mg	1.48	1.49	1.41	1.47
Co	0.02	0.00	0.00	0.00
Zn	0.00	0.00	0.03	0.00
Total	2.75	2.75	2.72	2.74

Table 3.Unit cell and X-ray diffraction collection parameters for six wadsleyites.

Parameter	SS1405Co	SS1406Ni	SS1406V	SS1407Cr	SS1407Zn	SS1405Ti
a	5.6913(3)	5.6739(5)	5.6604(6)	5.675(5)	5.7068(1)	5.6804(4)
b	11.4978(7)	11.5075(11)	11.5563(13)	11.4762(9)	11.4903(3)	11.4506(7)
c	8.2593(5)	8.2412(7)	8.2391(10)	8.2375(7)	8.2686(2)	8.2382(6)
Vol	540.4674	538.0878	538.9466	536.4872	542.1956	535.8507
b/*a*	2.0202	2.0281	2.0416	2.0222	2.0134	2.0158
2θ Max	74.70	70.24	64.86	64.81	69.56	80.12
#uniq	762	673	553	554	658	912
R merge	0.0272	0.0299	0.0358	0.0423	0.0442	0.0343
R final	0.0235	0.0459	0.0382	0.0372	0.0385	0.0268

Table 4. Atom position parameters for six wadsleyites.

Parameter	SS1405Co	SS1406Ni	SS1406V	SS1407Cr	SS1407Zn	SS1405Ti
M2						
Z	0.97043(8)	0.97149(18)	0.97102(17)	0.97102(16)	0.97032(16)	0.97025(11)
M3						
Y	0.12495(4)	0.12280(10)	0.12119(10)	0.12422(8)	0.12580(7)	0.12575(5)
T						
Y	0.12049(3)	0.12077(7)	0.12131(6)	0.12070(5)	0.12044(5)	0.12028(3)
Z	0.61616(4)	0.61579(10)	0.61532(9)	0.61589(8)	0.61647(9)	0.61633(5)
O1						
Z	0.22050(17)	0.22361(40)	0.22567(35)	0.22175(33)	0.22019(34)	0.21969(22)
O2						
Z	0.71602(16)	0.71614(37)	0.71570(32)	0.71676(32)	0.71664(33)	0.71668(21)
O3						
Y	0.98849(8)	0.98765(19)	0.98707(18)	0.98847(16)	0.98865(14)	0.98903(10)
Z	0.25598(11)	0.25596(24)	0.25619(24)	0.25595(21)	0.25582(22)	0.25579(14)
O4						
X	0.26089(10)	0.26098(25)	0.25986(26)	0.26076(22)	0.26128(19)	0.26078(15)
Y	0.12320(4)	0.12351(11)	0.12401(11)	0.12345(10)	0.12315(9)	0.12307(6)
Z	0.99361(8)	0.99416(17)	0.99508(16)	0.99391(16)	0.99319(16)	0.99344(10)

Table 5. Octahedral site geometry and occupancy parameters for six wadsleyites.

	SS1405Co	SS1406Ni	SS1406V	SS1407Cr	SS1407Zn	SS1405Ti
M1						
Mg (mol%)	95.7(3)	92.9(5)	99.8(9)	99.7(8)	97.3(4)	98.0(7)
TR (mol%)	4.3(3)	7.1(5)	0.2(9)	0.3(8)	2.7(4)	2.0(7)
M1-O3(2)	2.1184(9)	2.1142(20)	2.1161(20)	2.1125(17)	2.1193(18)	2.1110(12)
M1-O4(4)	2.0528(5)	2.0531(14)	2.054(14)	2.0493(12)	2.0564(11)	2.0453(8)
<M1-O>	2.0747	2.0734	2.0747	2.0704	2.0774	2.0673
PolyVol	11.8304(7)	11.8117(11)	11.8414(16)	11.7611(12)	11.8722(7)	11.7055(11)
M2						
Mg (mol%)	97.3(3)	97.4(5)	98.8(8)	99.8(2)	98.0(4)	98.2(7)
TR (mol%)	2.7(3)	2.6(5)	1.2(8)	0.2(2)	2.0(4)	1.8(7)
M2-O1	2.0654(15)	2.0778(37)	2.0981(31)	2.0654(29)	2.0661(31)	2.0550(20)
M2-O2	2.1012(14)	2.1044(35)	2.1036(29)	2.0945(28)	2.0976(31)	2.0889(19)
M2-O4(4)	2.0897(6)	2.0848(14)	2.0791(14)	2.082(12)	2.0937(11)	2.0841(8)
<M2-O>	2.0876	2.0869	2.0864	2.0813	2.0897	2.0801
PolyVol	12.0262(6)	12.0189(5)	11.9979(9)	11.9202(5)	12.0652(2)	11.8976(1)
M3						
Total Occ	92.4	87.6	79.7	91.2	96.6	95.2
Total Vacancy	7.6	12.4	20.2	8.8	3.5	4.8
Mg (mol%)	88.2(3)	83.1(4)	76.3(7)	89.4(7)	93.7(0)	92.4(0)
TR (mol%)	4.2(3)	4.5(4)	3.4(7)	1.8(7)	2.9(0)	2.8(0)
M3-O1(2)	2.0374(3)	2.0499(9)	2.0636(9)	2.0373(7)	2.0329(6)	2.0256(5)
M3-O3(2)	2.1186(7)	2.1055(18)	2.0994(18)	2.1077(15)	2.1263(13)	2.1141(10)
M3-O4(2)	2.1186(8)	2.1094(14)	2.1013(13)	2.1104(13)	2.1247(13)	2.1147(9)

<M3-O>	2.0916	2.0883	2.0881	2.0851	2.0946	2.0848
PolyVol	12.1033(3)	12.0599(3)	12.0581(2)	11.9996(1)	12.1558(1)	11.9838(3)
Vacancy (b/a)[a]	7.6	12.3	20.2	8.8	3.5	4.8

Note:TR =Transition metals

[a]calculated using equation: [vacancy]= ½ (b/a- 2.008) ×Si×M/11.25, M being the molar mass of the wadsleyite, see Smyth et al. (2014)

Table 6. Tetrahedral Site geometry and occupancy parameters for six wadsleyites.

	SS1405Co	SS1406Ni	SS1406V	SS1407Cr	SS1407Zn	SS1405Ti
Si (mol%)	97.6(4)	98.9(5)	97.3(7)	97.9(9)	99.5(3)	98.2(8)
TR (mol%)	2.4(4)	1.1(5)	2.7(7)	2.1(9)	0.5(3)	1.8(8)
Si-O2	1.7022(7)	1.7016(17)	1.7017(15)	1.7007(14)	1.7036(15)	1.7000(9)
Si-O3	1.6387(10)	1.6352(23)	1.6399(22)	1.6383(20)	1.6390(18)	1.6360(13)
Si-O4(2)	1.6355(7)	1.6313(15)	1.6358(15)	1.6317(13)	1.6368(12)	1.6326(9)
<Si-O>	1.6530	1.6499	1.6533	1.6506	1.6540	1.6502
PolyVol	2.3066(3)	2.2939(6)	2.3085(8)	2.2971(4)	2.3112(4)	2.2950(2)

Note:TR = Transition metals